Extracellular ATP acts on P2Y2 purinergic receptors to facilitate HIV-1 infection

Claire Séror,[1,3,4] Marie-Thérèse Melki,[5] Frédéric Subra,[6] Syed Qasim Raza,[1,3,4] Marlène Bras,[5] Héla Saïdi,[5] Roberta Nardacci,[7] Laurent Voisin,[1,3,4] Audrey Paoletti,[1,3,4] Frédéric Law,[1,3,4] Isabelle Martins,[1,3,4] Alessandra Amendola,[7] Ali A. Abdul-Sater,[8] Fabiola Ciccosanti,[7] Olivier Delelis,[6] Florence Niedergang,[10,11,13] Sylvain Thierry,[6] Najwane Said-Sadier,[8] Christophe Lamaze,[14] Didier Métivier,[1,3,4] Jérome Estaquier,[12,15] Gian Maria Fimia,[7] Laura Falasca,[7] Rita Casetti,[7] Nazanine Modjtahedi,[1,3,4] Jean Kanellopoulos,[16] Jean-François Mouscadet,[6] David M. Ojcius,[8,17] Mauro Piacentini,[7,9] Marie-Lise Gougeon,[5] Guido Kroemer,[1,2,13,18,19] and Jean-Luc Perfettini[1,3,4]

[1]Institut National de la Santé et de la Recherche Médicale (INSERM) U848 and [2]Metabolomics Platform, [3]Institut Gustave Roussy, F-94805 Villejuif, France
[4]Université Paris Sud - Paris 11, F-94805 Villejuif, France
[5]Antiviral Immunity, Biotherapy and Vaccine Unit, Department of Infection and Epidemiology, Institut Pasteur, F-75724 Paris Cedex 15, France
[6]Centre National de la Recherche Scientifique (CNRS) UMR 8113 LBPA, Ecole Normale Supérieure de Cachan, F-94230 Cachan, France
[7]National Institute for Infectious Diseases Lazzaro Spallanzani, 00149 Rome, Italy
[8]Health Sciences Research Institute and School of Natural Sciences, University of California, Merced, Merced, CA 95343
[9]Department of Biology, University of Rome Tor Vergata, 00173, Rome, Italy
[10]INSERM U1016, Institut Cochin, F-75016 Paris, France
[11]CNRS, UMR 8104, F-75014 Paris, France
[12]CNRS FRE3235, [13]Université Paris Descartes, F-75006 Paris, France
[14]UMR144 Curie/CNRS, Institut Curie, F-75248 Paris Cedex 05, France
[15]Centre de Recherche en Infectiologie, Université Laval, RC709 Québec, Canada
[16]UMR 8619, Université Paris Sud - Paris 11, F-91405 Orsay Cedex, France
[17]Université Paris Diderot, 75205 Paris Cedex 13, France
[18]Centre de Recherche des Cordeliers, F-75006 Paris, France
[19]Pôle de Biologie, Hôpital Européen Georges Pompidou, AP-HP, F-75908 Paris, France

CORRESPONDENCE
Jean-Luc Perfettini:
perfettini@orange.fr
OR
Guido Kroemer:
kroemer@orange.fr

Extracellular adenosine triphosphate (ATP) can activate purinergic receptors of the plasma membrane and modulate multiple cellular functions. We report that ATP is released from HIV-1 target cells through pannexin-1 channels upon interaction between the HIV-1 envelope protein and specific target cell receptors. Extracellular ATP then acts on purinergic receptors, including P2Y2, to activate proline-rich tyrosine kinase 2 (Pyk2) kinase and transient plasma membrane depolarization, which in turn stimulate fusion between Env-expressing membranes and membranes containing CD4 plus appropriate chemokine co-receptors. Inhibition of any of the constituents of this cascade (pannexin-1, ATP, P2Y2, and Pyk2) impairs the replication of HIV-1 mutant viruses that are resistant to conventional antiretroviral agents. Altogether, our results reveal a novel signaling pathway involved in the early steps of HIV-1 infection that may be targeted with new therapeutic approaches.

HIV-1 infection poses a public health problem that is partially controlled by a combination of specific antiretroviral agents. Nonetheless, the surge of multiresistant HIV-1 strains will require the development of novel antiviral strategies. Targeting early infection by vaccines and microbicides represents the main challenge to end the AIDS epidemic (Haase, 2010; Virgin and Walker, 2010).

Abbreviations used: CBX, carbenoxolone; DIDS, 4,4 diisothiocyanatostilbene-2,2′-disulfonic acid; HAART, highly active antiretroviral therapy; MDDC, monocyte-derived DC; MDM, monocyte-derived macrophage; MOI, multiplicity of infection; OxATP, oxidized ATP; PPADS, pyridoxal-phosphate-6-azophenyl-2′,4′-disulfonate; Pyk2, proline-rich tyrosine kinase 2; shRNA, short hairpin RNA; siRNA, small interfering RNA; SITS, 4-acetamido-4′-isothiocyanatostilbene-2,2′ disulfonic acid; VSV, vesicular stomatitis virus.

C. Séror, M.-T. Melki, and F. Subra contributed equally to this paper.
G. Kroemer and J.-L. Perfettini contributed equally to this paper.

The Rockefeller University Press $30.00
J. Exp. Med. Vol. 208 No. 9 1823-1834
www.jem.org/cgi/doi/10.1084/jem.20101805

The Journal of Experimental Medicine

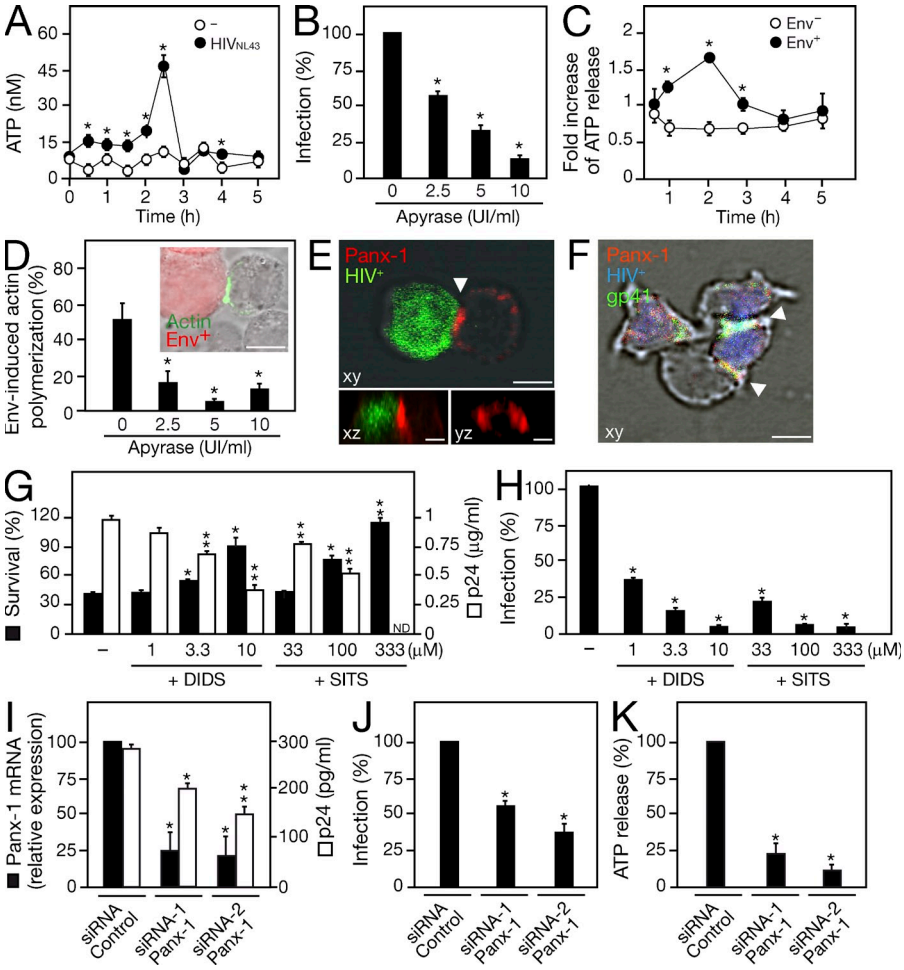

Figure 1. ATP release through pannexin-1 hemichannels modulates interactions of HIV-1 with target cells. (A) ATP released by CD4+CXCR4+ cells during HIV_{NL43} infection (MOI = 1; black circle) or in the absence of infection (white circle) was determined at different time points by ATP-dependent bioluminescence in three independent experiments. One representative experiment is shown (mean ± SEM of triplicates; *, $P < 0.01$). (B) CD4+CXCR4+ cells expressing a Tat-inducible β-galactosidase (β-gal) reporter gene were infected with HIV_{NL43} (MOI = 1) during 48 h in the presence of different concentrations of apyrase. Then, the medium containing apyrase was removed, replaced by complete medium, and target cell infection was determined 48 h after infection (mean ± SEM; three independent experiments; *, $P < 0.05$). (C) ATP release was expressed as a fold increase of ATP release during co-culture of HIV-1 target cells with Env+ or Env− cells. Error bars indicate SEM of three independent determinations (*, $P < 0.05$). (D) Effect of ATP depletion by apyrase on HIV-1 envelope mediated actin polymerization. Actin polymerization in pairs of interacting cells was determined in three independent experiments (means ± SEM; *, $P < 0.05$) by fluorescence microscopy. The inset illustrates actin polymerization (green) between an Env+ cell (red) and an interacting CD4+CXCR4+ cell (bar, 5 µm). (E) Localization of pannexin-1 at the contact site between primary HIV-1–infected lymphoblasts (green) and primary uninfected lymphoblasts, visualized by confocal microscopy. The arrowhead points to pannexin-1 accumulation (red) at the interface between primary infected and uninfected lymphoblasts (bar, 5 µm). A representative micrograph with merged images of xz (bar, 4 µm) and yz (bar, 1 µm) optical sections are shown. (F) Polarization of pannexin-1 (red) on the virological synapse between HIV-1–infected lymphoblasts (blue) and that of HIV-1–infected and uninfected cells. Arrowheads highlight the colocalization between pannexin-1 and the HIV-1 envelope glycoprotein gp41 (green; bar, 5 µm). The images in E and F are representative of at least 40 cells in three independent experiments. (G) CEM cells were infected during 6 d with HIV_{NL43} (MOI = 1) in the presence of different concentrations of DIDS or SITS. Effects on target cell survival and on p24 antigen release were determined. Error bars indicate SD of three independent determinations (*, $P < 0.01$; **, $P < 0.001$). (H) CD4+CXCR4+ cells expressing Tat-inducible β-gal reporter gene were infected with HIV_{NL43} (MOI = 1) during 3 h in the presence of the indicated concentrations of the indicated inhibitors. The medium was removed, replaced by complete medium, and target cell infectivity was determined (means ± SEM; $n = 3$; *, $P < 0.01$). (I) CD4+CXCR4+ cells were transfected during 48 h with siRNAs specific for pannexin-1 or control siRNA and then infected with HIV_{NL43} (MOI = 1). Pannexin-1 mRNA expression was measured by quantitative real-time RT-PCR. The effect of pannexin-1 depletion on p24 antigen release was determined as described in Materials and methods (means ± SEM; $n = 3$; *, $P < 0.01$; **, $P < 0.001$). (J and K) Cells were transfected with siRNA as in I. ATP release and HIV-1 infection were determined after 3 h (by ATP-dependent bioluminescence) and after 48 h (using CD4+CXCR4+ cells that contain a Tat-inducible β-Gal reporter), respectively. Results were obtained in three independent experiments (mean ± SEM; *, $P < 0.05$).

A better understanding of the early steps of HIV-1 infection is critical to achieving this goal. Enveloped viruses must fuse their membranes with host cell membranes to allow productive infection. Major transient changes in the charge and architecture of the host plasma membrane, including extreme curvature, occur during early steps of infection and facilitate viral replication (Miller et al., 1993; Davis et al., 2004). However, little is known about the consequences of these cell membrane alterations on the early signaling pathway required for viral infection.

Recent studies revealed that membrane stress induced by mechanical or chemical stimuli (shear stress [Wan et al., 2008], osmotic swelling [Darby et al., 2003], and membrane shrinking [Corriden and Insel, 2010]) stimulates ATP release. Initially described as a second messenger in the nervous and vascular systems (Schwiebert et al., 2002; Housley et al., 2009), extracellular ATP may also act as a proinflammatory mediator released during acute inflammation upon cell damage or bacterial infection, thus representing a generic marker of damage which can alert the immune system to danger (Gallucci and Matzinger, 2001). In addition, extracellular ATP inhibits infection by intracellular bacterial pathogens (Lammas et al., 1997; Coutinho-Silva et al., 2003) and modulates immune responses by participating in the chemotaxis of immune cells

(eosinophils, neutrophils, monocytes/macrophages, and immature DCs; Chen et al., 2006; Kronlage et al., 2010), by activating the NALP3 inflammasome (Mariathasan et al., 2006), or by mediating costimulatory signals for antigenic stimulation (Schenk et al., 2008). Recent studies revealed that ATP can also be released under basal conditions and influences a large array of cellular responses. Thus, ATP seems to act as an inside-out messenger that fine tunes signal transduction pathways (Corriden and Insel, 2010).

Outside of the cell, ATP acts as an autocrine/paracrine signal, modulating a variety of cellular functions by activating purinergic receptors (Corriden and Insel, 2010). These plasma membrane–localized receptors belong to a larger family that can be classified into ionotropic P2X receptor and metabotropic P2Y receptors (Ralevic and Burnstock, 1998). Metabotropic receptors are coupled to intracellular signaling pathways through heterotrimeric G proteins (Abbracchio et al., 2006), whereas ionotropic P2X receptors are associated with pores that open upon ATP binding, allowing Ca^{2+} influx and K^+ efflux (Ralevic and Burnstock, 1998). Seven members of the P2X family (P2X1–7; Ralevic and Burnstock, 1998) and eight P2Y receptors (P2Y1, P2Y2, P2Y4, P2Y6, P2Y11, P2Y12, P2Y13, and P2Y14) have been characterized (Abbracchio et al., 2003). Upon activation, these receptors, which are widely distributed throughout the body, modulate an array of cellular functions like plasma membrane permeabilization, Ca^{2+} influx, and cell death (Surprenant and North, 2009). Purinergic receptors have been extensively involved in the development of innate and/or adaptive immune responses against pathogens (Lammas et al., 1997; Coutinho-Silva et al., 2003; Chen et al., 2006; Mariathasan et al., 2006; Kronlage et al., 2010) but have also been associated with chemotherapy-driven anticancer immune responses (Ghiringhelli et al., 2009).

In this study, we determined whether ATP and purinergic receptors might modulate HIV-1 infection. We found that the HIV-encoded envelope glycoprotein complex (Env) can stimulate the release of ATP from HIV-1 target cells and that extracellular ATP then stimulates purinergic signals that facilitate HIV-1 infection. We characterized several elements of the signal transduction pathway—which facilitates ATP release from HIV-1 target cells and mediates autocrine ATP effects—that are essential for the early steps of HIV-1 infection.

RESULTS

ATP release from target cells participates in HIV-1 infection

Because membrane stress can induce the release of ATP from mammalian cells (Corriden and Insel, 2010), we speculated that HIV-1 infection might trigger ATP release from host cells. We found that infection of human cells with X4-tropic HIV-1 (HIV_{NL43}), which relies on the expression of CD4 and CXCR4 the receptor and co-receptor of HIV-1 (Dalgleish et al., 1984; Feng et al., 1996), led to rapid ATP release within the first 2 h of infection (Fig. 1 A). The depletion of CD4 by small interfering RNAs (siRNAs) or the inhibition of CXCR4 with its antagonist AMD3100 prevented ATP release (Fig. S1, A, B, E, and F). The addition of the nontoxic ATP-degrading enzyme apyrase

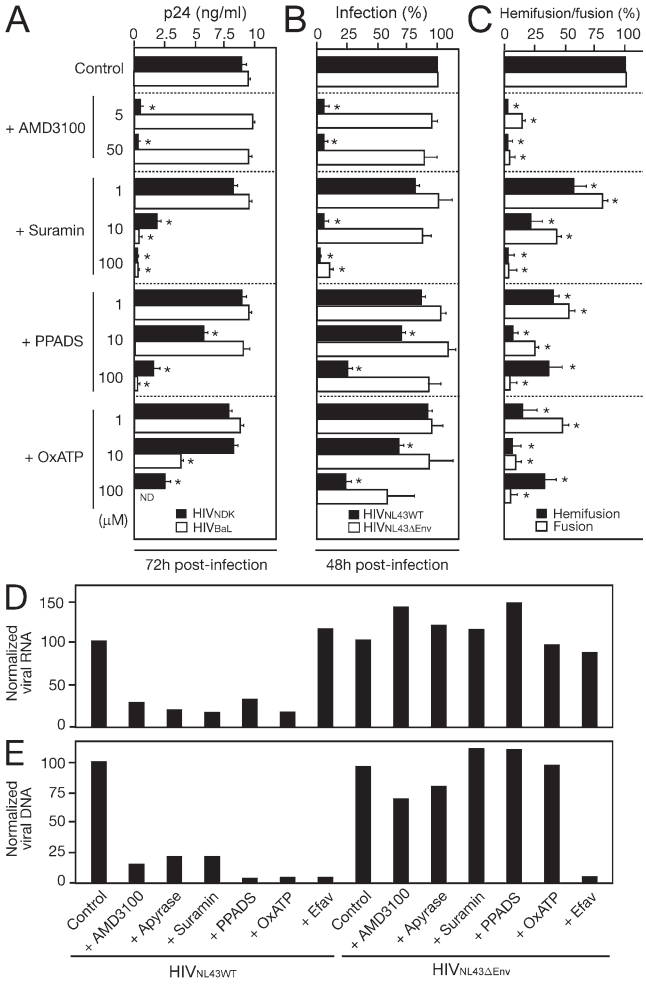

Figure 2. Purinergic receptors modulate HIV-1 infection. (A–C) Effects of CXCR4 receptor antagonist AMD3100 and the general P2 receptor antagonists suramin, PPADS, and OxATP on p24 release (A), host cell infectivity (B), and hemifusion/fusion (C), as observed during infection of PHA+IL-2–stimulated human PBMCs with HIV_{NDK} and HIV_{BaL} (A), during infection of $CD4^+CXCR4^+$ cells with HIV_{NL43WT} and $HIV_{NL43\Delta Env}$ (B), or during co-culture of Env^+ cells with HIV-1 target cells (C). Columns in A–C show means ± SEM ($n = 3$; *, $P < 0.05$). (D and E) Effects of 5 μM AMD3100, 10 UI/ml apyrase, 10 μM suramin, 100 μM PPADS, 100 μM OxATP, and 500 nM efavirenz (Efav) on viral RNA expression and on total viral DNA expression of wild-type (HIV_{NL43WT}) or VSVG pseudotyped ($HIV_{NL43\Delta Env}$) HIV-1 in $CD4^+CXCR4^+$ cells. Viral RNA was detected by quantitative PCR. Note that the internalization of pseudotyped $HIV_{NL43\Delta Env}$ virus was not reduced by these inhibitors (D). Total viral DNA was determined by PCR and results were normalized with respect to GAPDH (E). Efavirenz was used as an internal control of reverse transcription activity inhibition. The results are representative of three independent experiments.

(Fig. S1, A and D) prevented HIV-1 infection (Fig. 1 B), whereas supplementation with ATP or with its nonhydrolyzable analogue ATP-γS did not enhance HIV-1 infection (Fig. S1, C and D), perhaps because local ATP release is already optimal in the proximity of virions infecting cells. Co-culture of $CD4^+CXCR4^+$ cells with cells expressing the HIV-1 envelope glycoprotein complex (Env) at the plasma membrane also caused ATP release

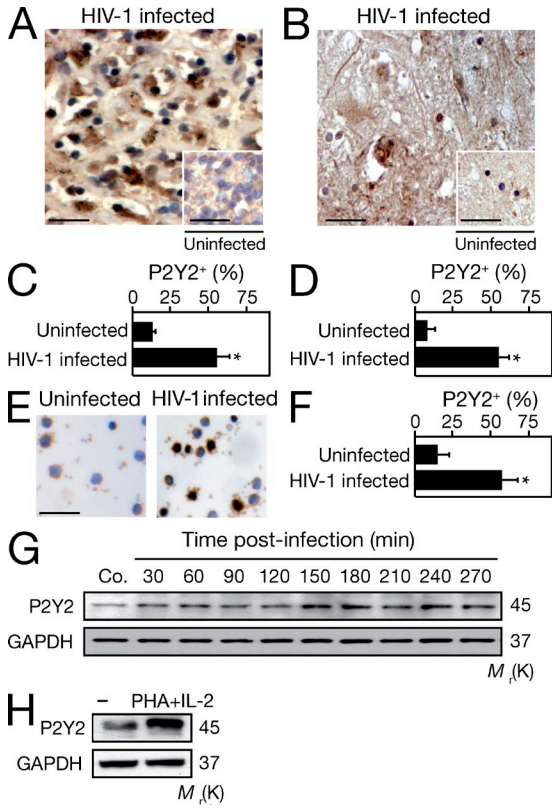

Figure 3. Detection of P2Y2 expression during HIV-1 infection. (A–D) Immunohistochemical P2Y2 detection in lymph node biopsies (A) and frontal cortex biopsies (B) obtained from HIV-1–infected patients. The insets illustrate the absence of staining in lymph node and frontal cortex biopsies from uninfected patients (bars, 50 µm). The percentage of $P2Y2^+$ cells was determined in lymph node (C) and frontal cortex (D) biopsies. Error bars represent means ± SEM ($n = 5$; *, $P < 0.01$). (E and F) P2Y2 detection in PBMCs obtained from uninfected or untreated HIV-1–infected patients. Representative microphotographs are shown in E (bars, 20 µm) and quantitative data are shown in F (mean ± SEM; $n = 3$; *, $P < 0.05$). (G) Primary lymphoblasts were infected with HIV_{NDK} (MOI=1) for the indicated periods. Then P2Y2 expression was evaluated by immunoblotting. Representative immunoblots of three independent experiments are shown. (H) Expression of P2Y2 on PBMC (−) and on PHA^+IL-2–activated PBMC was determined in three independent experiments and one representative immunoblot is shown.

as the cells were engaging in conjugates (Fig. 1 C). Apyrase abolished conjugate formation and the accompanying actin polymerization in juxtaposed cells (Fig. 1 D). The release of ATP from cells constitutes a common response to shear stress and osmotic imbalance (Wang et al., 2005) and can be mediated through mechanosensitive pannexin-1 hemichannels (Bao et al., 2004). Indeed, pannexin-1 was enriched at the contact site between HIV-1–infected lymphoblasts (which express Env on the surface) and uninfected lymphoblasts (Fig. 1 E). Pannexin-1 polarization occurred in conditions in which the levels of pannexin-1 protein remained constant (Fig. S1 G) and was preferentially detected in uninfected cells (Fig. S1, H and I). In addition, pannexin-1 was associated with virological synapses that formed between infected and uninfected cells (Fig. 1 F).

Pharmacological inhibition of pannexin-1 with 4,4 diisothiocyanatostilbene-2,2′-disulfonic acid (DIDS) or 4-acetamido-4′-isothiocyanatostilbene-2,2′ disulfonic acid (SITS) protected target cells against HIV-1–induced cell death (Fig. 1 G), reduced p24 antigen release (Fig. 1 G), and inhibited HIV-1 infection and fusion between CD4/CXCR4 and Env-expressing cells (Fig. 1 H; and Fig. S1, J and K). In these 6-d-long experiments, DIDS and SITS inhibited HIV-1 infection at doses that are lower than those required to prevent fusion between HIV Env^+ and $CD4^+CXCR4^+$ cells, perhaps reflecting cumulative effects over multiple viral cycles and/or distinct avidities (and hence susceptibilities to inhibition) of the interaction of infectable cells with HIV-1 Env present at the surface of cells versus viral particles. siRNA-mediated depletion of pannexin-1 from HIV-1 target cells also decreased p24 antigen release (Fig. 1 I), reduced HIV-1 infection (Fig. 1 J), blocked HIV-1 Env–mediated fusion (Fig. S1 L), and inhibited the release of ATP from host cells during conjugate formation (Fig. S1 L) and HIV-1 infection (Fig. 1 K). Thus, extracellular ATP release plays a major role in Env-dependent interactions between HIV-1 and host cells.

Purinergic receptors contribute to viral uptake

Extracellular ATP constitutes a common danger signal that is sensed by distinct purinergic receptors (Khakh and North, 2006). General inhibitors of purinergic receptors, including suramin, pyridoxal-phosphate-6-azophenyl-2′,4′-disulfonate (PPADS), and oxidized ATP (OxATP), blocked the replication of both X4-tropic HIV (e.g., HIV_{NDK}) and R5-tropic HIV (e.g., HIV_{BaL}) in activated T lymphoblasts (Fig. 2 A and Fig. S2 A). Purinergic receptor antagonists also blocked the replication of R5-tropic HIV-1 in macrophages (Fig. S2, B and C) or DCs (Fig. S2, D and E) and that of clinical HIV-1 isolates in C8166 T leukemia cells (Fig. S2, F–H).

Cervical epithelial (HeLa) cells engineered to express CD4/CXCR4, as well as a Tat-inducible β-galactosidase (β-Gal) reporter, expressed β-Gal upon infection with a lymphotropic HIV-1 (HIV_{NL43WT}). Such cells also expressed β-Gal upon infection by an isogenic virus in which the endogenous Env gene had been replaced by that of vesicular stomatitis virus (VSV; $HIV_{NL43\Delta Env}$) allowing the virus to infect cells which lack CD4/CXCR4 (Reiser et al., 1996). Purinergic receptor antagonists were more efficient in inhibiting β-Gal induction by Env-expressing than that by VSV-pseudotyped HIV-1 (Fig. 2 B and Fig. S3 A), indicating that they mainly affect the receptor-dependent facet of HIV-1 infection. Purinergic receptor inhibition also reduced the hemifusion (which causes the exchange of fluorescent lipids between interacting cells) and cell-to-cell fusion (syncytium formation with mixture of the cytoplasm) between $CD4^+CXCR4^+$ cells and Env-expressing cells (Fig. 2 C and Fig. S3 B). Finally, purinergic receptor antagonists prevented the entry of HIV-1 into cells, as revealed by their inhibitory effects on the detection of HIV genomes at the RNA (Fig. 2 D) and DNA (Fig. 2 E) levels within host cells. In contrast, purinergic receptor inhibition did not affect the replication of VSV-pseudotyped

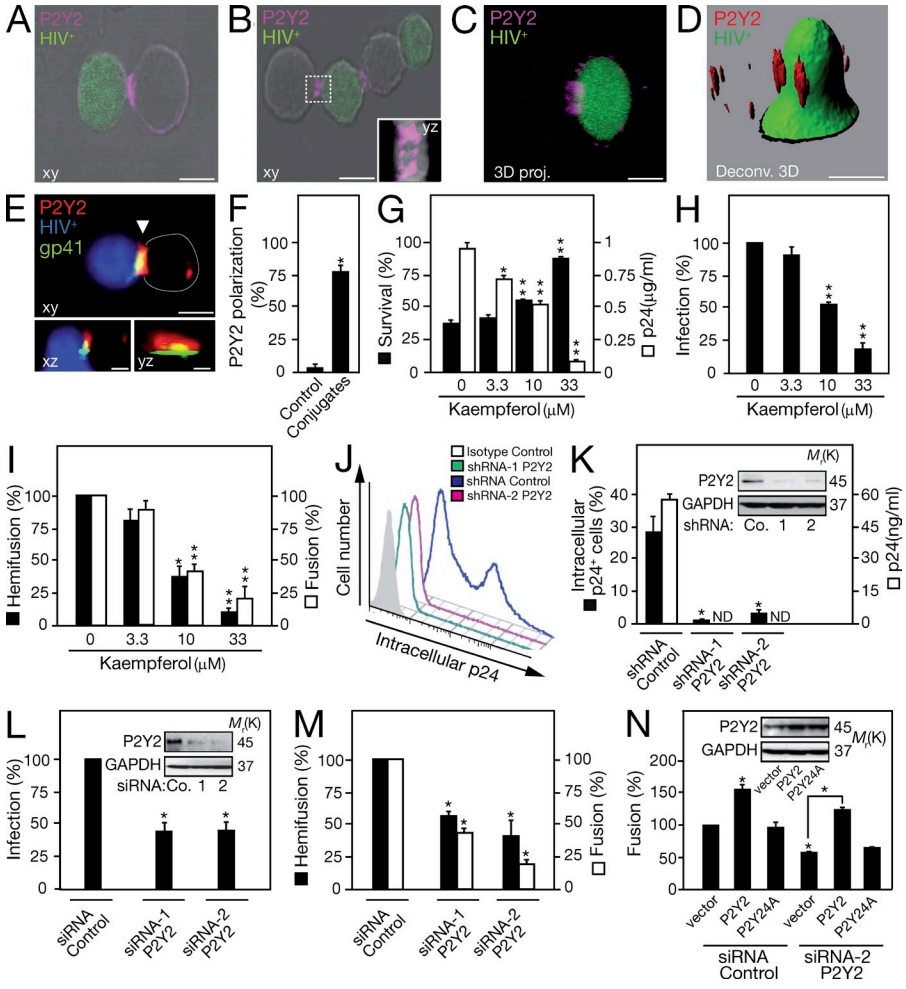

Figure 4. Role of P2Y2 in HIV-1 infection. (A–D) Detection of P2Y2 (pink, A–C; red, D) during the interaction between HIV-1–infected lymphoblasts (green) and uninfected lymphoblasts, as visualized by confocal microscopy. The inset in B represents a yz optical section and shows the circular distribution of P2Y2. Contrast phase in A and B revealed interacting lymphoblasts. 3D projection (C) and 3D reconstruction (D) of merged images unraveled a ring-like distribution of P2Y2 between interacting lymphoblasts (bars, 5 µm). (E) Detection of P2Y2 on virological synapse mediated by HIV-1 envelope between interacting lymphoblasts. Note the colocalization between P2Y2 (in red) and the HIV-1 envelope glycoprotein gp41 (in green) between HIV-1–infected lymphoblasts (in blue) and uninfected lymphoblasts (arrowhead). Representative micrographs of xy (bar, 5 µm), xz (bar, 4 µm), and yz (bar, 1 µm) optical sections are shown. Images in A–E are representative of at least four independent experiments. (F) Frequency of P2Y2 polarization at the virological synapse induced by HIV-1 between lymphoblasts. Data in F are means ± SEM of three independent experiments (*, $P < 0.05$). (G) Lymphocytic T CEM cells were infected during 6 d with HIV_{NL43} (MOI = 1) in the presence of different concentrations of the P2Y2 receptor antagonist kaempferol. Cell survival and p24 release were measured. Error bars indicate SD of three independent determinations (*, $P < 0.01$; **, $P < 0.001$). (H) $CD4^+CXCR4^+$ cells expressing Tat-inducible β-gal reporter gene were infected with HIV_{NL43} (MOI = 1) during 3 h in the presence of different kaempferol concentrations. 42 h after infection, the percentage of infected target cells was determined by β-Gal detection (mean ± SEM; $n = 3$; **, $P < 0.001$). (I) Effects of kaempferol on Env-induced hemifusion and fusion were determined after 24-h co-culture of $CD4^+CXCR4^+$ cells with Env^+ cells (means ± SD; $n = 3$; *, $P < 0.01$; **, $P < 0.001$). (J) Representative flow cytometric analysis of intracellular p24 antigen in HIV_{NDK}-infected CEM cells previously transduced with lentiviruses encoding indicated shRNA constructs. Representative profiles of three independent experiments are shown. (K) Cells were treated as in J and intracellular p24 and p24 release into the supernatant were determined (mean ± SD; $n = 3$; *, $P < 0.01$). ND, not detectable. P2Y2 expression by shRNA-transduced clones was evaluated by immunoblotting (inset). (L) $CD4^+CXCR4^+$ cells expressing Tat-inducible β-gal reporter gene were transfected during 48 h with siRNAs specific for P2Y2 or control siRNA and infected with HIV_{NL43} (MOI = 1). Then, target cell infectivity was determined (means ± SD; $n = 3$; *, $P < 0.01$). Insets show representative immunoblots of three independent experiments. (M) $CD4^+CXCR4^+$ cells were transfected with siRNA as in L. After 24 h of co-culture with HIV-1 Env^+ cells, hemifusion and fusion induced by HIV-1 envelope were determined (means ± SD; $n = 3$; *, $P < 0.01$). (N) $CD4^+CXCR4^+$ cells expressing Tat-inducible β-gal reporter gene were transfected with the indicated siRNA and with the wild-type P2Y2 or the P2Y2/4A mutant. Cell fusion mediated by the HIV-1 envelope was then evaluated by determining β-Gal activity during co-culture with HIV-1 Env^+ (mean ± SEM; $n = 3$; *, $P < 0.01$).

HIV-1 (Fig. 2, D and E). These results demonstrate that purinergic receptors are critical for the Env-mediated internalization of HIV-1 into suitable target cells.

Purinergic receptor P2Y2 modulates HIV-1 infection

To identify the principal purinergic receptors involved in HIV-1 internalization, we determined purinergic receptor expression on HIV-1 target cells (Fig. S4, A–N) and we selectively depleted the mRNAs coding for P2X1, P2X4, P2X7, P2Y1, P2Y2, and P2Y6 by siRNAs (Fig. S5, A–F). Depletion of P2Y2 consistently resulted in the strongest reduction in Env-triggered syncytium formation (Fig. S5 G). Immunoreactive P2Y2 was detectable at higher levels in lymphoid tissues (Fig. 3, A and C), in the frontal cortex (Fig. 3, B and D), and in circulating leukocytes (Fig. 3, E and F) from untreated HIV-1 carriers, as compared with uninfected carriers (Fig. 3, A, B, and E) and samples stained with isotype control antibody (Fig. S5, H and I). The levels of P2Y2 protein rapidly increased during in vitro HIV-1 infection of human PBMCs (Fig. 3 G), or $CD4^+CXCR4^+$ HeLa cells (Fig. S5 J), as well as after stimulation of human PBMCs with PHA and IL-2 (Fig. 3 H). Both HIV-1–infected and uninfected cells overexpressed P2Y2 (Fig. S6 A). Immunofluorescence microscopy

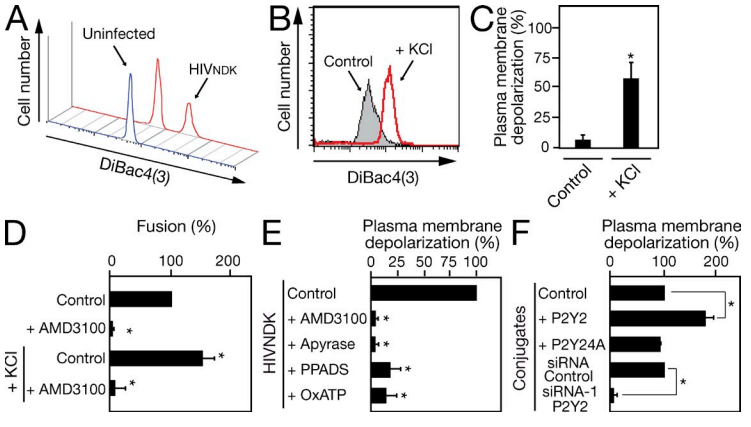

Figure 5. P2Y2 controls plasma membrane depolarization during HIV-1 Env–mediated fusion. (A) Plasma membrane depolarization of primary lymphoblasts 1 h after infection with HIV_{NDK} (MOI = 1) was determined by evaluating the increase of fluorescence of $DiBac_4(3)$ probe by flow cytometry. Representative profiles of three independent experiments are shown. (B) $CD4^+CXCR4^+$ cells were treated with 70 mM KCl or control for 3 h. Plasma membrane depolarization was determined by evaluating the increase of fluorescence of the $DiBac_4(3)$ probe. Representative profiles of three independent experiments are shown. (C) Frequency of plasma membrane depolarized $CD4^+CXCR4^+$ cells after 3 h of 70 mM KCl treatment (mean ± SEM; $n = 3$; *, $P < 0.05$). (D) Effects of 5 µM AMD3100 on HIV-1 Env–induced fusion in the absence or presence of 70 mM KCl. The error bars represent means ± SEM ($n = 3$; *, $P < 0.05$). (E) Effects of AMD3100, apyrase, PPADS, and OxATP on plasma membrane depolarization after 1 h of HIV_{NDK} infection. Results were obtained in three independent experiments (mean ± SEM; *, $P < 0.05$) using the $DiBac_4(3)$ probe and flow cytometry. (F) Effects of transfections of human P2Y2 wild-type (P2Y2), P2Y2 mutant (P2Y2/4A) constructs, and siRNA against P2Y2 (siRNA-1 P2Y2) on HIV-1 envelope–induced plasma membrane depolarization were determined as described in A (mean ± SEM; $n = 3$; *, $P < 0.05$).

revealed the polarization of P2Y2 at the contact site between HIV-1–infected and uninfected lymphoblasts (Fig. 4, A–F; and Fig. S6, B–D). P2Y2 distributed to ring-like structures (Fig. 4, B–E; and Fig. S6 E) that also contained the HIV-1 glycoprotein gp41 (Fig. 4 E) and the co-receptor CD4 (not depicted), indicating that P2Y2 accumulated at the virological synapse that is formed between HIV-1–infected and uninfected lymphoblasts. This P2Y2 polarization was observed preferentially in uninfected cells (Fig. 4 F and Fig. S6 E). Pharmacological P2Y2 inhibition with kaempferol (Kaulich et al., 2003; Fig. 4, G–I; and Fig. S6, F–H) or knockdown of P2Y2 (Fig. 4, J–M; and Fig. S6 I) reduced HIV-1–associated cell death (Fig. 4 G), HIV-1 infection (Fig. 4, G–L), and Env-mediated hemifusion and fusion (Fig. 4, I and M; and Fig. S6, G and H), suggesting that P2Y2 controls HIV-1 infection. Indeed, the transfection-enforced overexpression of P2Y2 increased the fusion between Env^+ and $CD4^+CXCR4^+$ cells (Fig. 4 N). In addition, the fusion-inhibitory effect of a P2Y2-specific siRNA was overcome by transfection with a non-interferable P2Y2 cDNA but not with a nonfunctional P2Y2 mutant, P2Y2/4A (Seye et al., 2004), underscoring the contribution of this purinergic receptor to HIV-1 infection (Fig. 4 N).

P2Y2 triggers plasma membrane depolarization to allow HIV-1 infection

Infection with HIV-1 is associated with a transient depolarization of the plasma membrane (Melikyan, 2008; Fig. 5 A). Transient abolition of the plasma membrane K^+ gradient by culturing cells in a medium containing 70 mM KCl for 3 h strongly induced membrane depolarization (Fig. 5, B and C) and enhanced the fusion of Env^+ and $CD4^+CXCR4^+$ cells that was reduced in the presence of the CXCR4 antagonist AMD3100 (Fig. 5 D), demonstrating that plasma membrane depolarization of HIV-1 target cells is required for Env-dependent fusion events. Plasma membrane depolarization induced by HIV-1 infection was abolished by addition of AMD3100, ATP-depleting apyrase, or several purinergic receptor antagonists (Fig. 5 E). To assess the involvement of P2Y2 in this event, we transfected $CD4^+CXCR4^+$ with a nonmutated P2Y2 cDNA (or as a control with the nonfunctional P2Y2/4A mutant) and observed that overexpression of functional P2Y2 increased the plasma membrane depolarization of $CD4^+CXCR4^+$ cells co-cultured with Env^+ cells (Fig. 5 F). Conversely, depletion of P2Y2 reduced HIV-1 Env–mediated plasma membrane depolarization (Fig. 5 F). These results demonstrate that the Src homology domain 3 binding sites (PxxP) of P2Y2 (which is mutated in the carboxy-terminal tail of P2Y2/4A) is required for plasma membrane depolarization and contributes to Env-dependent fusion events.

P2Y2-dependent activation of proline-rich tyrosine kinase 2 (Pyk2) is required for HIV-1 infection

P2Y2 (but not its mutant P2Y2/4A, see previous section) participates in the formation of a polyprotein complex that activates Pyk2 (Seye et al., 2004). We found that the activating phosphorylation or autophosphorylation on tyrosine residue 402 of Pyk2 (Pyk2Y402*) increased after P2Y2 overexpression during infection of human PBMCs with HIV-1 (Fig. 6 A) and during the formation of conjugates between Env^+ and $CD4^+CXCR4^+$ HeLa cells (Fig. S7 A). Pyk2Y402* overexpression was mainly detected in HIV-1–infected cells (Fig. S7 B). Moreover, Pyk2Y402* was enriched in ring-like structures at the contact site between such conjugates (Fig. 6, B and D) and between HIV-1–infected lymphoblasts and uninfected lymphoblasts (Fig. 6, C and E). In addition, Pyk2Y402* polarization was preferentially observed in uninfected lymphoblasts (Fig. S7 C). The phosphorylation of Pyk2 was also detectable in lymph nodes from untreated HIV-1 carriers (Fig. 6, F and H), in the frontal cortex from patients with HIV-associated encephalitis (HAE; Fig. 6, G and I), and in circulating leukocytes from HIV-1 carriers, correlating with viral load (Fig. 6 J). Approximately 40% of $CD3^+CD4^-$, 60% of $CD4^+$, and 15% of $CD19^+$ cells obtained from PBMCs revealed the activating phosphorylation of Pyk2 after in vitro

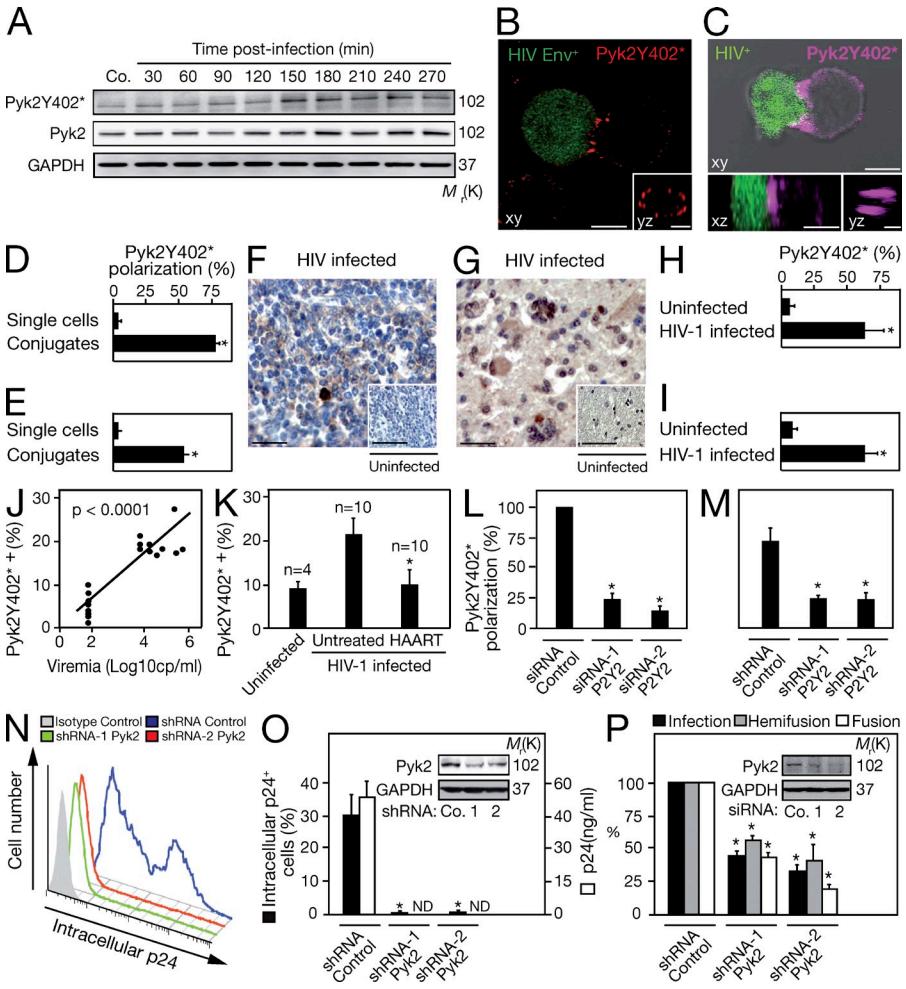

Figure 6. P2Y2 induces Pyk2 activation during HIV-1 infection. (A) PHA+IL-2–stimulated human PBMCs were infected with HIV_{NDK} (MOI = 1) for the indicated periods. Pyk2Y402* and Pyk2 expression were determined by immunoblotting. GAPDH expression was used as loading control. Representative immunoblots of three independent experiments are shown. (B) Representative Pyk2Y402* polarization (red) between HIV Env+ cells (green) and CD4+CXCR4+ cells was analyzed by confocal microscopy (bar, 5 µm). The inset in B shows the yz section (bar, 3 µm). (C) Detection of Pyk2Y402* (pink) polarization during interaction between HIV-1–infected lymphoblasts (green) and uninfected lymphoblasts by confocal microscopy (bar, 5 µm). The left inset represents an xz optical section and polarization of Pyk2Y402* between interacting cells (bar, 4 µm). The right inset corresponds to a yz optical section and shows peripheral distribution of Pyk2Y402* in the contact site within conjugates (bar, 3 µm). Images are representative of four independent experiments. (D and E) Frequency of Pyk2Y402* polarization between single cells and conjugates during co-culture of HIV Env+ cells and CD4+CXCR4+ cells (D) or co-culture of HIV-1–infected lymphoblasts and uninfected lymphoblasts (E) was determined in three independent experiments (mean ± SEM; *, $P < 0.05$). (F–I) Detection of Pyk2Y402* in lymph node sections (F and H) and frontal cortex biopsies (G and I) obtained from HIV-1–infected and uninfected patients (HIV-1–infected bar, 50 µm; HIV-1 uninfected bar, 25 µm). The percentage of Pyk2Y402*+ cells found in lymph node (H) and frontal cortex biopsies (I) was quantified. Error bars represent means ± SEM (*, $P < 0.01$; $n = 5$). (J) Correlation between Pyk2Y402* detected on PBMCs and viremia obtained from untreated HIV-1 carriers. The p-value corresponds to the correlation coefficient. (K) Effect of HAART on Pyk2Y402* detected on PBMCs obtained from treated patients, as compared with untreated HIV-1–infected donors (mean ± SEM; *, $P = 0.0009$). (L and M) Effects of P2Y2 knockdown on Pyk2Y402* polarization at the contact site between conjugates during co-culture of HIV Env+ cells and CD4+CXCR4+ cells (L) or co-culture of HIV-1–infected T CEM cells and uninfected P2Y2-depleted T CEM cells (M), as determined by confocal microscopy in three independent experiments (mean ± SEM; *, $P < 0.01$). (N and O) Effects of Pyk2 depletion on intracellular p24 (N and O) and p24 antigen release (O), as determined by immunofluorescence staining and ELISA, respectively. The indicated parameters were measured after HIV_{NDK} infection of CEM clones transduced with shRNAs specific for Pyk2, 6 d after infection. Representative FACS profiles of three independent experiments are shown in N and quantitative results (mean ± SD; $n = 3$; *, $P < 0.01$) are shown in O. (P) Effects of Pyk2 knockdowns on HIV_{NL43WT} infection, hemifusion, and fusion induced by HIV-1 envelope (mean ± SEM; $n = 3$; *, $P < 0.05$). The knockdown of Pyk2 by two nonoverlapping siRNAs was confirmed by Western blot (inset).

HIV-1 infection (Fig. S7 D). In addition, the vast majority of syncytia detected in lymph nodes from untreated HIV-1 carriers or in the frontal cortex from patients with HAE were positive for Pyk2Y402* (Fig. S7 E). Highly active antiretroviral therapy reduced immunodetectable Pyk2Y402* in PBMC from HIV-1–infected donors (Fig. 6 K). Depletion of P2Y2 reduced the phosphorylation of Pyk2 (Fig. S7 A) and inhibited the polarization of Pyk2Y402* at the contact sites between cocultured Env+ and CD4+CXCR4+ cells (Fig. 6 L) or between HIV-1–infected and uninfected target cells (Fig. 6 M and Fig. S7 F). Pyk2 depletion before HIV-1 infection similarly decreased intracellular p24 (Fig. 6, N and O; and Fig. S7 G) and p24 antigen release (Fig. 6 O), and Pyk2 knockdown inhibited HIV-1 infection, as well as Env-mediated hemifusion and fusion (Fig. 6 P). Collectively, these results indicate that Pyk2 is a critical effector of HIV-1 infection, operating downstream of P2Y2.

Depletion of each of the protein components of the hypothetical cascade delineated in this paper (pannexin-1→ATP→P2Y2→Pyk2) reduced infection by standard HIV-1 isolates (Fig. 1, B, I, and J; Fig. 4, J–L; and Fig. 6, N–P) as well as by viruses that had been rendered resistant against reverse transcription and integrase inhibitors by selective point mutations (Bacheler et al., 2000; Delelis et al., 2009; Fig. 7 A).

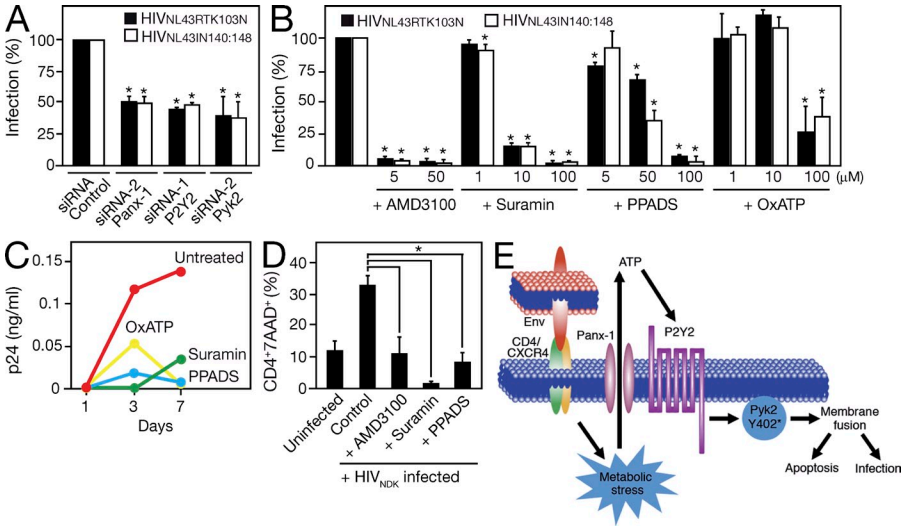

Figure 7. Inhibition of pannexin-1, P2Y2, and Pyk2 reduces HIV-1 infectivity and T cell depletion associated with HIV-1 infection. (A) Effects of pannexin-1, P2Y2, and Pyk2 siRNA on the infectious activity of therapy-resistant HIV-1 mutated viruses ($HIV_{NL43RTK103N}$ and $HIV_{NL43IN140:148}$). Target cell infectivity was determined using $CD4^+CXCR4^+$ cells expressing Tat-inducible β-Gal reporter gene. Results are representative of three independent experiments (mean ± SEM; *, $P < 0.01$). (B) Effects of different concentrations of suramin, PPADS, and OxATP on HIV mutant infectivity, as determined in A. (C) $PH2^+IL\text{-}2$–stimulated PBMCs obtained from HAART-treated patients (with undetectable viremia) were treated with 100 µM suramin, 100 µM PPADS, and 100 µM OxATP. Then, p24 antigen release was determined after 1, 3, and 7 d of infection. Results shown are representative of three HAART-treated patients. (D) HIV_{NDK}-infected $PHA^+IL\text{-}2$–stimulated lymphoblasts were treated with 5 µM AMD3100, 100 µM suramin, or 100 µM PPADS. 7-AAD uptake (analyzed by flow cytometry) and intracellular p24 antigen expression (measured by flow cytometry) were assessed. Results were pooled from three independent experiments (mean ± SEM; *, $P < 0.01$). (E) Involvement of pannexin-1, ATP release, P2Y2 activation, and Pyk2Y402* phosphorylation in early stages of HIV-1 infection. Binding of HIV-1 envelope to cellular receptors leads to rapid ATP release from host cells through pannexin-1. ATP then activates P2Y2 receptors, leading to activation (phosphorylation) of Pyk2 (Pyk2Y402*). P2Y2 and Pyk2 control plasma membrane depolarization, hemifusion, and fusion, which are required for HIV-1 infection.

Similarly, purinergic receptor antagonists were able to inhibit infection by genetically engineered therapy-resistant HIV-1 mutants (Fig. 7 B) and tritherapy-selected viruses (Fig. 7 C), consistent with the possibility that inhibition of the pannexin-1→ATP→P2Y2→Pyk2 cascade can mediate antiretroviral effects under conditions in which conventional therapy fails. In addition, purinergic receptor antagonists reduced the death of activated $CD4^+$ T lymphoblasts infected by HIV-1 (Fig. 7 D), suggesting that interruption of P2Y2 signaling confers immunoprotective effects.

DISCUSSION

Although many early steps of infectious processes are associated with host membrane alterations, there are no studies that evaluate whether extracellular nucleotides might impact on the viral life cycle. In this paper, we show that ATP is released into the extracellular milieu during the early steps of HIV-1 infection and that this extracellular ATP is required for efficient viral uptake. During the initial stages of the infectious process, ATP release may determine viral clearance or the persistence of the infection by effects on the immune system. Massive ATP release during infection reportedly can deliver a danger signal to immune effectors. Thus, extracellular ATP may activate the inflammasome, which participates in the caspase-1–dependent maturation and secretion of the proinflammatory cytokines IL-1β, IL-18, and IL-33 (Schroder and Tschopp, 2010) or stimulate neutrophil migration and phagocytosis (Chen et al., 2006). Moreover, extracellular ATP can favor the killing of some intracellular pathogens (Lammas et al., 1997; Coutinho-Silva et al., 2003) or, on the contrary, promote the survival of other infectious agents (Corriden and Insel, 2010). Thus, a recent study revealed that OppA, the substrate-binding domain of *Mycoplasma hominis* permease increases the microbe's extracellular survival by inducing release of ATP from host cells (Hopfe and Henrich, 2008). In addition, treatment of *Mycobacterium avium*–infected cells with apyrase decreased intracellular survival of the pathogens (Woo et al., 2007). Our results differ from these studies in that they demonstrate that extracellular ATP released by HIV-1 host cells favors the initial steps of HIV-1 infection. Thus, ATP that is rapidly released during the infectious process from HIV-1 target cells does not only act as a danger signal but also contributes to viral uptake.

In this paper, we report the identification of proteins involved in HIV-1–induced ATP release and in ATP-mediated signaling events that contribute to viral infection. Thus, we identified several novel proteins that are required for efficient HIV-1 infection of $CD4^+$ host cells and showed that HIV-1 can stimulate ATP release into the extracellular milieu through pannexin-1 hemichannels, perhaps as a result of mechanical stress of the host cell membrane (Bao et al., 2004). ATP then acts in an autocrine and paracrine fashion to activate purinergic receptors, in particular P2Y2, a seven-transmembrane-anchored G protein–coupled receptor that can induce the phosphorylation/recruitment of the proline/tyrosine kinase Pyk2 (Liu et al., 2004). Indeed, pannexin-1, P2Y2, and Pyk2 were all recruited to the contact site between Env-containing and CD4/CXCR4-containing membranes, suggesting that they act within the virological synapse to transduce signals that enhance membrane-to-membrane fusion, participate in the infectious process, and facilitate viral cell-to-cell transmission (Fig. 7 E; Jolly et al., 2007; Hübner et al., 2009).

At present, the exact mechanisms by which P2Y2 modulates HIV-1 infection remain elusive. However, we found that after the interaction between HIV-1 envelope and its co-receptors, P2Y2 was activated and could directly interact with filamin A, a modulator of the actin cytoskeleton involved in the formation of stable receptor–co-receptor complexes (Jiménez-Baranda et al., 2007). P2Y2 can also indirectly, through its SH3 binding (PxxP) site, control the phosphorylation of Pyk2 on tyrosine 402 (Liu et al., 2004), and this event might induce its phosphorylation/relocation to the virological synapse. Pyk2 regulates multiple signaling events that participate in the reorganization of the actin cytoskeleton and contribute to macrophage polarization and migration in response to chemokine stimulation (Okigaki et al., 2003). Pyk2 can control HIV-1 Env–mediated fusion (Harmon and Ratner, 2008). During HIV-1 infection, Pyk2 is phosphorylated after interactions between distinct Env variants (from X4- and R5-tropic strains) and Env receptors on HIV-1 target cells (CD4 and chemokine receptors; Davis et al., 1997). The activating phosphorylation or autophosphorylation of Pyk2 (Pyk2Y402*) that we detected during HIV-1 infection in vitro and in vivo might be induced in response to chemokine stimulation or elevations of intracellular Ca^{2+} concentrations (Lev et al., 1995). Activated Pyk2 then may modulate the formation of a signaling complex that contains Src family kinases and actin interacting proteins (Block et al., 2010). In this paper, we identified the ATP-mediated stimulation of the purinergic receptor P2Y2 as an upstream event required for the phosphorylation of Pyk2 (Pyk2Y402*). P2Y2 activation is known to modulate Ca^{2+} influx after nucleotide binding (Ralevic and Burnstock, 1998) and may also regulate Pyk2 activities by recruiting it into a polyprotein complex that also contains the tyrosine kinase Src (Seye et al., 2004). Although we demonstrated that P2Y2 activation induced Pyk2Y402*, the precise mechanisms linking P2Y2 activation and polarization/phosphorylation of Pyk2 remain elusive. Moreover, future investigations must explore how plasma membrane depolarization, which is essential for HIV-1 infection, results from the activation of P2Y2 and Pyk2.

Inhibition of any of the constituents of the molecular cascade that we delineated in this study (pannexin-1→ATP→P2Y2→Pyk2) could interrupt the HIV-1 life cycle at the level of viral entry. Thus, inhibition of pannexin hemichannels, enzymatic depletion of extracellular ATP, antagonizing P2Y2 receptors, or suppression of Pyk2 kinase activity could constitute effective strategies for the blockade of HIV-1 infection, be it locally (for instance by application of topical gels) or systemically (ideally with orally available drugs). The toxicology of some putative therapeutic agents acting on this cascade (such as apyrase) is satisfactory (Marcus et al., 2005), whereas that of others (such as suramin) is not (Grossman et al., 2001), underlining the need for the development of highly specific inhibitors against pannexin-1, P2Y2, and Pyk2. Beyond these clinical considerations, it will be important to investigate whether any or all of the constituents of the pannexin-1→ATP→P2Y2→Pyk2 pathway may participate in host cell infection by HIV-1–unrelated viruses.

MATERIALS AND METHODS

Cells and culture conditions. PBMCs were isolated from the blood of normal volunteers (Etablissement Français du Sang [EFS] Cabanel, Paris, France) over a Ficoll-Hypaque density gradient. Blood was obtained through the EFS in the setting of EFS-Institut Pasteur Convention. A written informed consent was obtained for each donor to use the cells for clinical research in compliance with French Law and the Biomedical Research Committee Board from Institut Pasteur (Paris, France). $CD14^+$ monocytes were isolated from PBMC by positive selection using anti-CD14 beads (Miltenyi Biotec). To generate monocyte-derived macrophages (MDMs), purified monocytes were incubated in RPMI 1640 medium supplemented with 100 U/ml penicillin–100 µg/ml streptomycin (Invitrogen) and 10% FCS in the presence of 10 ng/ml recombinant human (rh) M-CSF (Pepro Tech). After 6 d of culture, adherent cells corresponding to the macrophage-enriched fraction were harvested, washed, and used for subsequent experiments. To generate monocyte-derived DCs (MDDCs), purified monocytes were cultured in RPMI 1640 medium supplemented with 10% antibiotics and FCS. Cultures were maintained for 6 d in 24-well trays (10^6 cells/well) supplemented with 10 ng/ml rhGM-CSF (PeproTech) and rhIL-4 (PeproTech). The medium was replaced every 2 d. After 6 d of culture, MDDCs were semi-adherent cells and expressed high levels of DC-SIGN but not monocyte/macrophage markers such as CD14 and CD16. Flow cytometry analysis (CellQuest software; BD) demonstrated that MDMs and MDDCs were >90% pure. T cells were subsequently prepared from the monocyte-depleted cell fractions. PBLs were cultured for 48 h in fresh medium supplemented with 2.5 µg/ml PHA (Sigma-Aldrich) and 1 µg/ml rhIL-2 (PeproTech). PBLs were then washed and cultured in growth medium containing 1 µg/ml rhIL-2 for 24 h. These cells were infected with HIV-1 during 3 d with a multiplicity of infection (MOI) of 1, as previously described (Saïdi et al., 2008; Melki et al., 2010). HeLa cells stably transfected with the Env gene of HIV-1 LAI/IIIB (HeLa Env) and HeLa cells transfected with CD4 (HeLa CD4) were cultured alone or together at a 1:1 ratio in Dulbecco's modified Eagle's medium supplemented with 10% FCS, 2 mM L-glutamine, and 100 UI/ml penicillin/streptomycin (Invitrogen) in the absence or in presence of tested molecules. CEM T lymphocytes were maintained in RPMI 1640 medium containing 10% FCS, 2 mM L-glutamine, and 100 UI/ml penicillin/streptomycin (Invitrogen).

Viral and pseudo-viral constructs. Viral stocks of wild-type X4, R5, and resistant HIV-1 were obtained after transfection of 293T with virus encoding plasmids as previously described (Perfettini et al., 2008; Delelis et al., 2009). The standardization of HIV-1 infection was achieved by means of the Alliance HIV-1 P24 antigen ELISA assay (PerkinElmer) and infection of P4 cells followed by fixation and determination of β-galactosidase activity. Viral RNA and DNA and viral production were analyzed, as previously described (Delelis et al., 2009).

Pharmacological inhibitions. Primary human lymphoblasts, MDMs, MDDCs, lymphocytic CEM cells, or $CD4^+CXCR4^+$ target cells were seeded into 96-well culture plates ($1–2 \times 10^4$ cells /well) and incubated 30 min with increasing concentrations of apyrase, CXCR4 antagonist (AMD3100), the P2 receptor antagonist suramin, the P2X-selective antagonist OxATP, the P2Y-selective antagonist PPADS, carbenoxolone (CBX), DIDS, and SITS. Then, cells were incubated with wild-type HIV-1, VSV-pseudotyped HIV-1, therapy-resistant HIV-1 mutated viruses (1 ng of p24 antigen), or clinical HIV-1 isolates (15 ng of p24 antigen) for 3 h at 37°C in a 5% CO_2 atmosphere. After washing out unabsorbed virus, cells were cultured for the indicated times in the presence of tested molecules. The absolute number of total remaining viable cells and cell death were analyzed, as previously described (Lecoeur et al., 2002; Melki et al., 2010). Apyrase, AMD3100, ATP, ATP-γS, suramin, PPADS, OxATP, CBX, DIDS, and SITS were purchased from Sigma-Aldrich.

RNA interference. siRNAs specific for pannexin-1 (siRNA-1, 5′-GCUCCAAGGUAUGAACAUA-3′; siRNA-2, 5′-ACGAUUUGAGCCUCUACAA-3′), CD4 (siRNA, 5′-ACUGAGGAGUCUCUUGAUC-3′),

P2X1 (siRNA, 5′-GUGGCAGUCAGUAACCAUA-3′), P2X4 (siRNA, 5′-GGAAAACUCCCUCUUCGUC-3′), P2X7 (siRNA, 5′-GCUGUCG-CUCCCAUAUUUA-3′), P2Y1 (siRNA, 5′-AUUAUCACCAGGUAAAUG-GAUUUCC-3′), P2Y2 (siRNA-1, 5′-GGAUAGAAGAUGUGUUGGG-3′; siRNA-2, 5′-GGCUGUAACUUAUACUAAA-3′), P2Y6 (siRNA, 5′-GG-UGCUCACAAAAAUACA-3′), PYK2 (siRNA-1, 5′-GCUGAUCGGCAU-CAUUGAA-3′; siRNA-2, 5′-GGCGGUUCUUCAAGGAUAU-3′), and control sirRNA (5′-GCCGGUAUGCCGGUUAAGU-3′) were transfected 48 h before HIV-1 infection or cell fusion using Oligofectamine (Invitrogen), according to the manufacturer's instructions. For short hairpin RNA (shRNA) lentiviral particle transduction, the pRS shRNA expression retroviral vector coding for each targeted gene was purchased from Origene. Oncovirus vector particles were generated by cotransfection of three plasmids coding for the gag-pol genes from moloney mouse leukemia virus (pUMVC3-gag-pol; University of Michigan), for the vector genome carrying your shRNA of interest (pRS shRNA), and for the plasmid coding for an envelope of VSV (pMDG; Tronolab). Cotransfection was effected into 293T cells (human embryonic kidney cell) using superFect transfection reagent (QIAGEN) according to the manufacturer's protocol.

On day 2 after transfection, supernatants were filtered (0.45-µm cellulose acetate filters; Sartorius Stedim), aliquoted, and frozen at −80°C. For transduction, oncovirus aliquots were added to T lymphocytic CEM-T4 cell line, and 24 h after infection the medium was replaced with fresh growth medium containing 1 µg/ml puromycin (Cayla). Clonal populations were obtained by transferring single cells into U-bottom 96-well plates and by maintaining selection pressure for 3 wk. Silencing of proteins was determined by quantitative RT-PCR and/or by Western blotting.

Quantitative real-time RT-PCR. mRNA was isolated from cells after the indicated treatments using the RNeasy kit (QIAGEN) according to the manufacturer's instructions, and total RNA was converted into cDNA by standard reverse transcription with the TaqMan reverse transcription kit (Applied Biosystems). Quantitative PCR were performed with the cDNA preparation (1:50) in the Mx3000P system (Agilent Technologies) in a 25-µl final volume with Brilliant QPCR Master Mix (Agilent Technologies). The primers for human for human Panx-1 were 5′-GGTGAGACAAGACCCAGAGC-3′ (forward) and 5′-GGCATCGGACCTTACACCTA-3′ (reverse). The primers for human P2X1 were 5′-GCTGGTGCGTAATAAGAAGGTG-3′ (forward) and 5′-ATGAGGCCGCTCGAGGTCTG-3′ (reverse). The primers for human P2X4 were 5′-GATACCAGCTCAGGAGGAAAAC-3′ (forward) and 5′-GCATCATAAATGCACGACTTGAG-3′ (reverse). The primers for human P2X7 were 5′-TGATAAAAGTCTTCGGGATCCGT-3′ (forward) and 5′-TGGACAAATCTGTGAAGTCCATC-3′ (reverse). The primers for human P2Y1 were 5′-CTTGGTGCTGATTCTGGGCTG-3′ (forward) and 5′-GCTCGGGAGAGTCTCCTTCTG-3′ (reverse). The primers for human P2Y2 were 5′-CCGCTCGCTGGACCTCAGCTG-3′ (forward) and 5′-CTCACTGCTGCCCAACACATC-3′ (reverse). The primers for human P2Y4 were 5′-CGCTGCCCACCCTCATCTAC-3′ (forward) and 5′-CCGAGTGGTGTCATGGCACAG-3′ (reverse). The primers for human P2Y5 were 5′-TGTTCAGTCTACCCACTCTCAG-3′ (forward) and 5′-CTTACTGCTGCCACTACTGAGC-3′ (reverse). The primers for human P2Y6 were 5′-AACCTTGCTCTGGCTGACCTG-3′ (forward) and 5′-GCAGGCACTGGGTTGTCACG-3′ (reverse). The primers for human P2Y8 were 5′-CTCCTGGCGCACATCGTGAG-3′ (forward) and 5′-GGAGCGCACGGACGTGGTC-3′ (reverse). The primers for human P2Y10 were 5′-GGTGTTCATGTGTGCTGCAGTC-3′ (forward) and 5′-ATGGCGGGATAGTTGGTCACG-3′ (reverse). The primers for human P2Y11 were 5′-GAGGCCTGCATCAAGTGTCTG-3′ (forward) and 5′-ACGTTGAGCACCCGCATGATG-3′ (reverse). The primers for human P2Y12 were 5′-ACCGGTCATACGTAAGAACGAG-3′ (forward) and 5′-GCAGAATTGGGGCACTTCAGC-3′ (reverse). The primers for human P2Y13 were 5′-GGAAGCAACACCATCGTCTGTG-3′ (forward) and 5′-GACTGTGAGTATATGGAACTCTG-3′ (reverse) and for human GAPDH were 5′-CAATGCATCCTGCACCACCAA-3′ (forward) and 5′-GTCATTGAGAGCAATGCCAGC-3′ (reverse). Real-time PCR included initial denaturation at 95°C for 10 min, followed by 40 cycles at 95°C for 30 s, 55°C for 1 min, and 72°C for 1 min, and one cycle at 95°C for 1 min, 55°C for 30 s, and 95°C for 30 s. The CT values were normalized to the housekeeping gene GAPDH.

Immunoblots, immunofluorescence, and flow cytometry. Total cellular proteins were extracted in 250-mM NaCl-containing lysis buffer (250 mM NaCl, 0.1% NP-40, 5 mM EDTA, 10 mM Na_3VO_4, 10 mM NaF, 5 mM DTT, 3 mM $Na_4P_2O_7$, and the protease inhibitor cocktail [EDTA-free protease inhibitor tablets; Roche]). 50 µg of protein extracts were run on 4–12% SDS-PAGE and transferred at 4°C onto a nitrocellulose membrane. After blocking, membranes were incubated with primary antibody at room temperature overnight. Horseradish peroxidase–conjugated goat anti–mouse or anti–rabbit (SouthernBiotech) antibodies were then incubated for 1 h and revealed with the enhanced ECL detection system. After 3 d of infection with HIV_{NDK} (MOI = 1), PHA/IL-2–stimulated peripheral blood lymphocytes were stained with 10 µM 5-chloromethylfluorescein diacetate (Cell Tracker green; CMFDA; Invitrogen) and cocultured with uninfected lymphoblasts for 48 h. Cells were then fixed in 4% paraformaldehyde/PBS for 30 min, permeabilized in 0.1% SDS in PBS, and incubated with FCS for 20 min, as previously described (Perfettini et al., 2004). Polyclonal rabbit antibodies for the detection of P2Y2 were purchased from Abcam or Alomone laboratories. Polyclonal rabbit antibodies against pannexin-1 were obtained from Abcam and Millipore. The polyclonal rabbit antibodies used for the detection of Pyk2 and the phosphorylated form of Pyk2 on tyrosine 402 (Pyk2Y402*) were obtained from Cell Signaling Technology. The monoclonal mouse antibody against HIV-1 gp41 (50–69) was obtained from National Institutes of Health AIDS Research and Reference Reagent Program (Bethesda, MD). Antisera were used for immunodetection in PBS containing 1 mg/ml BSA and revealed with goat anti–rabbit IgG conjugated to Alexa Fluor 546 fluorochromes from Invitrogen. Actin was also stained using an Alexa Fluor 647 (or 488)–conjugated phalloidin depending on the experiment. Cells were analyzed by fluorescent confocal microscopy on an LSM510 (Carl Zeiss) using a 63× objective. Z series of optical sections at 0.2-µm increments were acquired. After image deconvolution, 3 D image reconstructions of interacting cells were performed using the IsoSurface function of Imaris 5.7 Software (Bitplane AG). Phenotypic analyses were realized by flow cytometry as previously described (Melki et al., 2010), and we used the monoclonal mouse antibody against HIV-1 p24 (KC57) conjugated to FITC (Beckman Coulter), the monoclonal mouse antibodies against CD3 or CD4 conjugated to FITC or to peridinin chlorophyll protein complex (PerCP; BD), and the monoclonal mouse antibody against CD19 conjugated to allophycocyanin (Miltenyi Biotech).

Measurement of extracellular ATP. ATP release during co-cultures or infection with HIV-1 were determined using the Enliten ATP assay system (Promega) as described by the manufacturer. The luminescence was measured by integration over a 3-s time interval using the luminometer Fluostar OPTIMA (BMG Labtech).

Hemifusion and cell–cell fusion assays. HeLa Env^+ and HeLa $CD4^+CXCR4^+$ cells were, respectively stained for hemifusion analysis with 1 µM 1,1′-dioctadecyl-3,3,3′,3′-tetramethylindocarbocyanine perchlorate ($DiIC_{18}(3)$, Invitrogen) and 10 µM 5-chloromethylfluorescein diacetate (Cell Tracker green; CMFDA) or for cell–cell fusion analysis, respectively, with 10 µM 5-chloromethylfluorescein diacetate (Cell Tracker green; CMFDA) and 10 µM 5-,6-,4-chloromethylbenzoyl aminotetramethyl rhodamine (Cell Tracker orange; CMTMR; Invitrogen). Cells were then cultured alone or together for 24 h, at a 1:1 ratio in Dulbecco's modified Eagle's medium supplemented with 10% FCS, 2 mM L-glutamine, and penicillin/streptomycin (Invitrogen) in the absence or presence of the indicated concentrations of purinergic receptor inhibitors. The effects of these inhibitors on hemifusion and cell–cell fusion mediated by the HIV-1 envelope were evaluated by fluorescence microscopy.

Measurement of target cell infectability. HeLa cells stably transfected with CD4, as well as the LacZ gene under the control of the HIV-1 LTR (HeLa-CD4), were selected in medium containing 500 µg/ml G418. Target

cell infectability was evaluated using HeLa-CD4$^+$CXCR4$^+$ cells. After 2 d of infection, cells were lysed and β-galactosidase activity was measured using the enhanced β-galactosidase assay kit (CPRG; Gene Therapy Systems).

Plasma membrane depolarization detection. PHA/IL-2–stimulated human lymphoblasts were stained with 300 nM $DiBac_4(3)$ (Invitrogen) for 20 min at 37°C. Cells were then infected with HIV_{NDK} (at an MOI of 1) for 1 h. We then measured the depolarization-associated increase of $DiBac_4(3)$ fluorescence intensity by flow cytometry. Propidium iodide uptake was used to exclude necrotic cells from the analysis of $DiBac_4(3)$ fluorescence. Using the same procedure, we analyzed plasma membrane depolarization induced by the HIV-1 envelope.

Patients. Peripheral blood samples were obtained from healthy and HIV-1–infected individuals (all males, mean age 36 yr) in accordance with the Italian and EU legislations, after approval by the Institutional Review Board of the National Institute for Infectious Disease Lazzaro Spallanzani. Patients were naive for highly active antiretroviral therapy (HAART) with a plasma viral load >20,000 copies/ml or were receiving HAART with a viral load <5,000 copies/ml. Plasma HIV-1 RNA levels were determined by the Abbott Real-time HIV-1 assay according to the manufacturer's instructions (Abbott Molecular). PBMCs of HIV-1–infected patients were obtained from residual samples intended to HIV RNA quantification for routine clinical management and were isolated by Ficoll/Hypaque (GE Healthcare) centrifugation of heparinized blood from either healthy donors or HIV-seropositive individuals and fixed with 4% paraformaldehyde in PBS, pH 7.2. PBMCs from HAART-treated patients that had undetectable virus in the plasma were used for ex vivo experiments. The amounts of endogenous virus produced and used during these ex vivo experiments were monitored by using Vironostika HIV-1 Antigen assay according to the manufacturer's instructions (Biomerieux).

Immunohistochemical analysis. Biopsies from axillary lymph nodes and from postmortem frontal cortex were obtained in accordance with the Italian and EU legislations, after approval by the Institutional Review Board of the National Institute for Infectious Disease Lazzaro Spallanzani. Human tissue sections in paraffin were deparaffinized, rehydrated, and subjected to high-temperature antigen retrieval in 10 mM sodium citrate buffer, pH 6.0. Endogenous peroxidase activity was blocked by 3% H_2O_2. Rabbit antibody against P2Y2 (Alomone laboratories) or Pyk2Y402* (Abcam) and biotinylated goat anti–rabbit IgG were incubated with tissue sections. Immunoreaction product obtained with a preformed horseradish peroxidase–conjugated streptavidin (Biogenex) was revealed using aminoethylcarbazole as chromogenic substrates and 0.01% H_2O_2 (Biogenex). Sections were then counterstained in Mayer's acid hemalum. The lymph node and brain cortex sections obtained from HIV-infected patients were evaluated by three independent observers using a light microscope. For each slide, a minimum of 10 fields was examined at 40× magnification.

Statistical analysis. To determine statistical significance, Student's *t* test was used for calculation of p-values.

Online supplemental material. Fig. S1 demonstrates pannexin-1–dependent ATP release during HIV-1 infection and during HIV-1 Env–mediated fusion. Fig. S2 shows the impact of P2 inhibitors on cell viability, viral production, host cell infectivity, and hemifusion/fusion during HIV-1 infection. Fig. S3 shows effects of P2 inhibitors on co-cultured Env$^+$ and CD4$^+$CXCR4$^+$ HeLa cells. Fig. S4 reveals purinergic receptor and pannexin-1 expression on human PBMCs and on PHA/IL-2–stimulated PBMC. Fig. S5 shows the identification of purinergic receptors involved in HIV-1 Env–mediated fusion and controls for immunohistochemical analyses. Fig. S6 shows the detection of polarized P2Y2 at the virological synapse mediated by HIV_{NDK}. Fig. S7 shows that Pyk2 is activated during HIV-1 infection. Online supplemental material is available at http://www.jem.org/cgi/content/full/jem.20101805/DC1.

We thank the National Institutes of Health AIDS Research and Reference Reagent Program (Bethesda, MD) and Laurie Erb (Bond Life Sciences Center, USA) for reagents, and A. Jalil (Institut National de la Santé et de la Recherche Médicale U753, France) and O. Duc (Institut Gustave Roussy, France) for technical help.

This work has been supported by a grant from Sidaction (to J.-L. Perfettini), as well as grants from Agence Nationale des Recherches sur le Sida et sur les hépatites virales, La Ligue Nationale contre le Cancer, Sidaction, and the European Commission (RIGHT, ACTIVE P53, ApoSys, ArtForce; to G. Kroemer) and Istituto Superiore di Sanità (no. 40F60, Ricerca Corrente e Finalizzate "Ministerio della Saluté", COFIN from Ministro dell'Istruzione, dell'Università e della Ricerca and Associazione Italiana per la Ricerca sul Cancro).

The authors declare no conflicting financial interests.

Submitted: 31 August 2010
Accepted: 27 July 2011

REFERENCES

Abbracchio, M.P., J.M. Boeynaems, E.A. Barnard, J.L. Boyer, C. Kennedy, M.T. Miras-Portugal, B.F. King, C. Gachet, K.A. Jacobson, G.A. Weisman, and G. Burnstock. 2003. Characterization of the UDP-glucose receptor (re-named here the P2Y14 receptor) adds diversity to the P2Y receptor family. *Trends Pharmacol. Sci.* 24:52–55. doi:10.1016/S0165-6147(02)00038-X

Abbracchio, M.P., G. Burnstock, J.M. Boeynaems, E.A. Barnard, J.L. Boyer, C. Kennedy, G.E. Knight, M. Fumagalli, C. Gachet, K.A. Jacobson, and G.A. Weisman. 2006. International Union of Pharmacology LVIII: update on the P2Y G protein-coupled nucleotide receptors: from molecular mechanisms and pathophysiology to therapy. *Pharmacol. Rev.* 58:281–341. doi:10.1124/pr.58.3.3

Bacheler, L.T., E.D. Anton, P. Kudish, D. Baker, J. Bunville, K. Krakowski, L. Bolling, M. Aujay, X.V. Wang, D. Ellis, et al. 2000. Human immunodeficiency virus type 1 mutations selected in patients failing efavirenz combination therapy. *Antimicrob. Agents Chemother.* 44:2475–2484. doi:10.1128/AAC.44.9.2475-2484.2000

Bao, L., S. Locovei, and G. Dahl. 2004. Pannexin membrane channels are mechanosensitive conduits for ATP. *FEBS Lett.* 572:65–68. doi:10.1016/j.febslet.2004.07.009

Block, E.R., M.A. Tolino, and J.K. Klarlund. 2010. Pyk2 activation triggers epidermal growth factor receptor signaling and cell motility after wounding sheets of epithelial cells. *J. Biol. Chem.* 285:13372–13379. doi:10.1074/jbc.M109.083089

Chen, Y., R. Corriden, Y. Inoue, L. Yip, N. Hashiguchi, A. Zinkernagel, V. Nizet, P.A. Insel, and W.G. Junger. 2006. ATP release guides neutrophil chemotaxis via P2Y2 and A3 receptors. *Science.* 314:1792–1795. doi:10.1126/science.1132559

Corriden, R., and P.A. Insel. 2010. Basal release of ATP: an autocrine-paracrine mechanism for cell regulation. *Sci. Signal.* 3:re1. doi:10.1126/scisignal.3104re1

Coutinho-Silva, R., L. Stahl, M.N. Raymond, T. Jungas, P. Verbeke, G. Burnstock, T. Darville, and D.M. Ojcius. 2003. Inhibition of chlamydial infectious activity due to P2X7R-dependent phospholipase D activation. *Immunity.* 19:403–412. doi:10.1016/S1074-7613(03)00235-8

Dalgleish, A.G., P.C. Beverley, P.R. Clapham, D.H. Crawford, M.F. Greaves, and R.A. Weiss. 1984. The CD4 (T4) antigen is an essential component of the receptor for the AIDS retrovirus. *Nature.* 312:763–767. doi:10.1038/312763a0

Darby, M., J.B. Kuzmiski, W. Panenka, D. Feighan, and B.A. MacVicar. 2003. ATP released from astrocytes during swelling activates chloride channels. *J. Neurophysiol.* 89:1870–1877. doi:10.1152/jn.00510.2002

Davis, C.B., I. Dikic, D. Unutmaz, C.M. Hill, J. Arthos, M.A. Siani, D.A. Thompson, J. Schlessinger, and D.R. Littman. 1997. Signal transduction due to HIV-1 envelope interactions with chemokine receptors CXCR4 or CCR5. *J. Exp. Med.* 186:1793–1798. doi:10.1084/jem.186.10.1793

Davis, H.E., M. Rosinski, J.R. Morgan, and M.L. Yarmush. 2004. Charged polymers modulate retrovirus transduction via membrane charge neutralization and virus aggregation. *Biophys. J.* 86:1234–1242. doi:10.1016/S0006-3495(04)74197-1

Delelis, O., I. Malet, L. Na, L. Tchertanov, V. Calvez, A.G. Marcelin, F. Subra, E. Deprez, and J.F. Mouscadet. 2009. The G140S mutation in HIV integrases from raltegravir-resistant patients rescues catalytic defect due

to the resistance Q148H mutation. *Nucleic Acids Res.* 37:1193–1201. doi:10.1093/nar/gkn1050

Feng, Y., C.C. Broder, P.E. Kennedy, and E.A. Berger. 1996. HIV-1 entry cofactor: functional cDNA cloning of a seven-transmembrane, G protein-coupled receptor. *Science*. 272:872–877. doi:10.1126/science.272.5263.872

Gallucci, S., and P. Matzinger. 2001. Danger signals: SOS to the immune system. *Curr. Opin. Immunol.* 13:114–119. doi:10.1016/S0952-7915(00)00191-6

Ghiringhelli, F., L. Apetoh, A. Tesniere, L. Aymeric, Y. Ma, C. Ortiz, K. Vermaelen, T. Panaretakis, G. Mignot, E. Ullrich, et al. 2009. Activation of the NLRP3 inflammasome in dendritic cells induces IL-1beta-dependent adaptive immunity against tumors. *Nat. Med.* 15:1170–1178. doi:10.1038/nm.2028

Grossman, S.A., S. Phuphanich, G. Lesser, J. Rozental, L.B. Grochow, J. Fisher, and S. Piantadosi; New Approaches to Brain Tumor Therapy CNS Consortium. 2001. Toxicity, efficacy, and pharmacology of suramin in adults with recurrent high-grade gliomas. *J. Clin. Oncol.* 19:3260–3266.

Haase, A.T. 2010. Targeting early infection to prevent HIV-1 mucosal transmission. *Nature*. 464:217–223. doi:10.1038/nature08757

Harmon, B., and L. Ratner. 2008. Induction of the Galpha(q) signaling cascade by the human immunodeficiency virus envelope is required for virus entry. *J. Virol.* 82:9191–9205. doi:10.1128/JVI.00424-08

Hopfe, M., and B. Henrich. 2008. OppA, the ecto-ATPase of Mycoplasma hominis induces ATP release and cell death in HeLa cells. *BMC Microbiol.* 8:55. doi:10.1186/1471-2180-8-55

Housley, G.D., A. Bringmann, and A. Reichenbach. 2009. Purinergic signaling in special senses. *Trends Neurosci.* 32:128–141. doi:10.1016/j.tins.2009.01.001

Hübner, W., G.P. McNerney, P. Chen, B.M. Dale, R.E. Gordon, F.Y. Chuang, X.D. Li, D.M. Asmuth, T. Huser, and B.K. Chen. 2009. Quantitative 3D video microscopy of HIV transfer across T cell virological synapses. *Science*. 323:1743–1747. doi:10.1126/science.1167525

Jiménez-Baranda, S., C. Gómez-Moutón, A. Rojas, L. Martínez-Prats, E. Mira, R. Ana Lacalle, A. Valencia, D.S. Dimitrov, A. Viola, R. Delgado, et al. 2007. Filamin-A regulates actin-dependent clustering of HIV receptors. *Nat. Cell Biol.* 9:838–846. doi:10.1038/ncb1610

Jolly, C., I. Mitar, and Q.J. Sattentau. 2007. Adhesion molecule interactions facilitate human immunodeficiency virus type 1-induced virological synapse formation between T cells. *J. Virol.* 81:13916–13921. doi:10.1128/JVI.01585-07

Kaulich, M., F. Streicher, R. Mayer, I. Müller, and C.E. Müller. 2003. Flavonoids — novel lead compounds for the development of P2Y2 receptor antagonists. *Drug Dev. Res.* 59:72–81. doi:10.1002/ddr.10203

Khakh, B.S., and R.A. North. 2006. P2X receptors as cell-surface ATP sensors in health and disease. *Nature*. 442:527–532. doi:10.1038/nature04886

Kronlage, M., J. Song, L. Sorokin, K. Isfort, T. Schwerdtle, J. Leipziger, B. Robaye, P.B. Conley, H.C. Kim, S. Sargin, et al. 2010. Autocrine purinergic receptor signaling is essential for macrophage chemotaxis. *Sci. Signal.* 3:ra55. doi:10.1126/scisignal.2000588

Lammas, D.A., C. Stober, C.J. Harvey, N. Kendrick, S. Panchalingam, and D.S. Kumararatne. 1997. ATP-induced killing of mycobacteria by human macrophages is mediated by purinergic P2Z(P2X7) receptors. *Immunity*. 7:433–444. doi:10.1016/S1074-7613(00)80364-7

Lecoeur, H., L.M. de Oliveira-Pinto, and M.L. Gougeon. 2002. Multiparametric flow cytometric analysis of biochemical and functional events associated with apoptosis and oncosis using the 7-aminoactinomycin D assay. *J. Immunol. Methods*. 265:81–96. doi:10.1016/S0022-1759(02)00072-8

Lev, S., H. Moreno, R. Martinez, P. Canoll, E. Peles, J.M. Musacchio, G.D. Plowman, B. Rudy, and J. Schlessinger. 1995. Protein tyrosine kinase PYK2 involved in Ca(2+)-induced regulation of ion channel and MAP kinase functions. *Nature*. 376:737–745. doi:10.1038/376737a0

Liu, J., Z. Liao, J. Camden, K.D. Griffin, R.C. Garrad, L.I. Santiago-Pérez, F.A. González, C.I. Seye, G.A. Weisman, and L. Erb. 2004. Src homology 3 binding sites in the P2Y2 nucleotide receptor interact with Src and regulate activities of Src, proline-rich tyrosine kinase 2, and growth factor receptors. *J. Biol. Chem.* 279:8212–8218. doi:10.1074/jbc.M312230200

Marcus, A.J., M.J. Broekman, J.H. Drosopoulos, K.E. Olson, N. Islam, D.J. Pinsky, and R. Levi. 2005. Role of CD39 (NTPDase-1) in thromboregulation, cerebroprotection, and cardioprotection. *Semin. Thromb. Hemost.* 31:234–246. doi:10.1055/s-2005-869528

Mariathasan, S., D.S. Weiss, K. Newton, J. McBride, K. O'Rourke, M. Roose-Girma, W.P. Lee, Y. Weinrauch, D.M. Monack, and V.M. Dixit. 2006. Cryopyrin activates the inflammasome in response to toxins and ATP. *Nature*. 440:228–232. doi:10.1038/nature04515

Melikyan, G.B. 2008. Common principles and intermediates of viral protein-mediated fusion: the HIV-1 paradigm. *Retrovirology*. 5:111. doi:10.1186/1742-4690-5-111

Melki, M.T., H. Saïdi, A. Dufour, J.C. Olivo-Marin, and M.L. Gougeon. 2010. Escape of HIV-1-infected dendritic cells from TRAIL-mediated NK cell cytotoxicity during NK-DC cross-talk—a pivotal role of HMGB1. *PLoS Pathog.* 6:e1000862. doi:10.1371/journal.ppat.1000862

Miller, M.A., M.W. Cloyd, J. Liebmann, C.R. Rinaldo Jr., K.R. Islam, S.Z. Wang, T.A. Mietzner, and R.C. Montelaro. 1993. Alterations in cell membrane permeability by the lentivirus lytic peptide (LLP-1) of HIV-1 transmembrane protein. *Virology*. 196:89–100. doi:10.1006/viro.1993.1457

Okigaki, M., C. Davis, M. Falasca, S. Harroch, D.P. Felsenfeld, M.P. Sheetz, and J. Schlessinger. 2003. Pyk2 regulates multiple signaling events crucial for macrophage morphology and migration. *Proc. Natl. Acad. Sci. USA*. 100:10740–10745. doi:10.1073/pnas.1834348100

Perfettini, J.L., T. Roumier, M. Castedo, N. Larochette, P. Boya, B. Raynal, V. Lazar, F. Ciccosanti, R. Nardacci, J. Penninger, et al. 2004. NF-κB and p53 are the dominant apoptosis-inducing transcription factors elicited by the HIV-1 envelope. *J. Exp. Med.* 199:629–640. doi:10.1084/jem.20031216

Perfettini, J.L., R. Nardacci, M. Bourouba, F. Subra, L. Gros, C. Séror, G. Manic, F. Rosselli, A. Amendola, P. Masdehors, et al. 2008. Critical involvement of the ATM-dependent DNA damage response in the apoptotic demise of HIV-1-elicited syncytia. *PLoS ONE*. 3:e2458. doi:10.1371/journal.pone.0002458

Ralevic, V., and G. Burnstock. 1998. Receptors for purines and pyrimidines. *Pharmacol. Rev.* 50:413–492.

Reiser, J., G. Harmison, S. Kluepfel-Stahl, R.O. Brady, S. Karlsson, and M. Schubert. 1996. Transduction of nondividing cells using pseudotyped defective high-titer HIV type 1 particles. *Proc. Natl. Acad. Sci. USA*. 93:15266–15271. doi:10.1073/pnas.93.26.15266

Saïdi, H., M.T. Melki, and M.L. Gougeon. 2008. HMGB1-dependent triggering of HIV-1 replication and persistence in dendritic cells as a consequence of NK-DC cross-talk. *PLoS ONE*. 3:e3601. doi:10.1371/journal.pone.0003601

Schenk, U., A.M. Westendorf, E. Radaelli, A. Casati, M. Ferro, M. Fumagalli, C. Verderio, J. Buer, E. Scanziani, and F. Grassi. 2008. Purinergic control of T cell activation by ATP released through pannexin-1 hemichannels. *Sci. Signal.* 1:ra6. doi:10.1126/scisignal.1160583

Schroder, K., and J. Tschopp. 2010. The inflammasomes. *Cell*. 140:821–832. doi:10.1016/j.cell.2010.01.040

Schwiebert, L.M., W.C. Rice, B.A. Kudlow, A.L. Taylor, and E.M. Schwiebert. 2002. Extracellular ATP signaling and P2X nucleotide receptors in monolayers of primary human vascular endothelial cells. *Am. J. Physiol. Cell Physiol.* 282:C289–C301.

Seye, C.I., N. Yu, F.A. González, L. Erb, and G.A. Weisman. 2004. The P2Y2 nucleotide receptor mediates vascular cell adhesion molecule-1 expression through interaction with VEGF receptor-2 (KDR/Flk-1). *J. Biol. Chem.* 279:35679–35686. doi:10.1074/jbc.M401799200

Surprenant, A., and R.A. North. 2009. Signaling at purinergic P2X receptors. *Annu. Rev. Physiol.* 71:333–359. doi:10.1146/annurev.physiol.70.113006.100630

Virgin, H.W., and B.D. Walker. 2010. Immunology and the elusive AIDS vaccine. *Nature*. 464:224–231. doi:10.1038/nature08898

Wan, J., W.D. Ristenpart, and H.A. Stone. 2008. Dynamics of shear-induced ATP release from red blood cells. *Proc. Natl. Acad. Sci. USA*. 105:16432–16437. doi:10.1073/pnas.0805779105

Wang, E.C., J.M. Lee, W.G. Ruiz, E.M. Balestreire, M. von Bodungen, S. Barrick, D.A. Cockayne, L.A. Birder, and G. Apodaca. 2005. ATP and purinergic receptor-dependent membrane traffic in bladder umbrella cells. *J. Clin. Invest.* 115:2412–2422. doi:10.1172/JCI24086

Woo, S.R., R.G. Barletta, and C.J. Czuprynski. 2007. Extracellular ATP is cytotoxic to mononuclear phagocytes but does not induce killing of intracellular Mycobacterium avium subsp. paratuberculosis. *Clin. Vaccine Immunol.* 14:1078–1083. doi:10.1128/CVI.00166-07